Journal of Inflammation Research

Dovepress
Taylor & Francis Group

Open Access Full Text Article

ORIGINAL RESEARCH

Inhibition of CD53 Reduces the Formation of ROS-Induced Neutrophil Extracellular Traps and Protects Against Inflammatory Injury in Acute Pancreatitis

Tianqi Xia[1,2], Fei Han[1,2], Yaning Wang[1,2], Xinyue Xie[1,2], Chenchen Yuan[1,2], Guotao Lu[1,2], Weiming Xiao[1,2], Bo Tu[3], Hongbo Ren[4], Weijuan Gong[1,2], Yaodong Wang[5]

[1]Pancreatic Center, Department of Gastroenterology, the Affiliated Hospital of Yangzhou University, Yangzhou University, Yangzhou, 225000, People's Republic of China; [2]Yangzhou Key Laboratory of Pancreatic Disease, the Affiliated Hospital of Yangzhou University, Yangzhou University, Yangzhou, 225000, People's Republic of China; [3]Clinical Research Division, Fred Hutchinson Cancer Research Center, Seattle, WA, USA; [4]Department of Gastroenterology, Qilu Hospital, Shandong University, Jinan, Shandong Province, 250012, People's Republic of China; [5]Department of Gastroenterology, Kunshan Hospital of Traditional Chinese Medicine, Suzhou Key Laboratory of Integrated Traditional Chinese and Western Medicine of Digestive Diseases, Kunshan Affiliated Hospital of Yangzhou University, Kunshan, 215300, People's Republic of China

Correspondence: Yaodong Wang; Weijuan Gong, Email day.wang@live.cn; wjgong@yzu.edu.cn

Background: The tetraspanin CD53 transmembrane protein is vital in immune cells like B cells and T cells, playing a crucial role in various inflammatory conditions. However, its involvement in neutrophils regarding inflammation remains uncertain. This study aims to examine the impact of CD53 on neutrophil extracellular traps (NETs) formation.

Methods: Phorbol 12-myristate 13-acetate (PMA) was utilized to establish an in vitro classical NETs model to investigate the influence of CD53 on NETs formation and its regulatory mechanisms. Subsequently, the link between CD53 and acute pancreatitis (AP), a model of aseptic inflammatory responses connected to NETs, was verified. Peripheral blood neutrophils from clinical AP patients were collected to explore the role of CD53 in AP, while an AP mouse model induced by caerulein was employed to confirm the impact of CD53 inhibition on AP mice pancreatic tissue.

Results: Our study has shown that CD53 is significantly elevated in in vitro NETs models and neutrophils from AP patients. The expression of CD53 is closely related to the clinical prognosis of AP patients. At the same time, CD53 neutralizing antibody (Anti-CD53) can significantly inhibit the formation of NETs in vitro, inflammatory injury in AP mice and the formation of NETs in damaged tissues. Mechanistically, CD53 can modulate the PI3K/AKT pathway and promote the formation of NETs. Finally, targeted regulation of CD53 can effectively reduce inflammatory injury and NETs formation in damaged tissues of AP mice.

Conclusion: The results of this study mark the first confirmation that CD53 plays a crucial role in NETs formation. Targeting CD53 inhibition could potentially serve as a novel therapeutic approach for the treatment of AP.

Keywords: CD53, neutrophil extracellular traps, acute pancreatitis, PI3K/AKT

Introduction

Acute pancreatitis (AP) is a pancreatic inflammatory condition characterized by the inappropriate activation of digestive enzymes, resulting in autodigestion of pancreatic acinar cells.[1,2] Most cases of mild acute pancreatitis (MAP) are self-limiting. Repeated or excessive acinar cell injury releases a large number of pro-inflammatory mediators and inflammatory chemokines while causing pancreatic necrosis, and secondary pancreatic necrosis infection, systemic inflammatory response and multiple organ failure can progress to SAP, which is a dangerous condition with a mortality rate of up to 20–40%.[3,4] The dysregulation of the immune system is pivotal in the progression and pathology of SAP.[5] Early studies indicate that immune cells help control pancreatic inflammation by capturing microorganisms and releasing bactericidal enzymes. Failure to regulate this immune response promptly can exacerbate pancreatic injury, leading to systemic

Received: 21 November 2024
Accepted: 4 March 2025
Published: 13 March 2025

Graphical Abstract

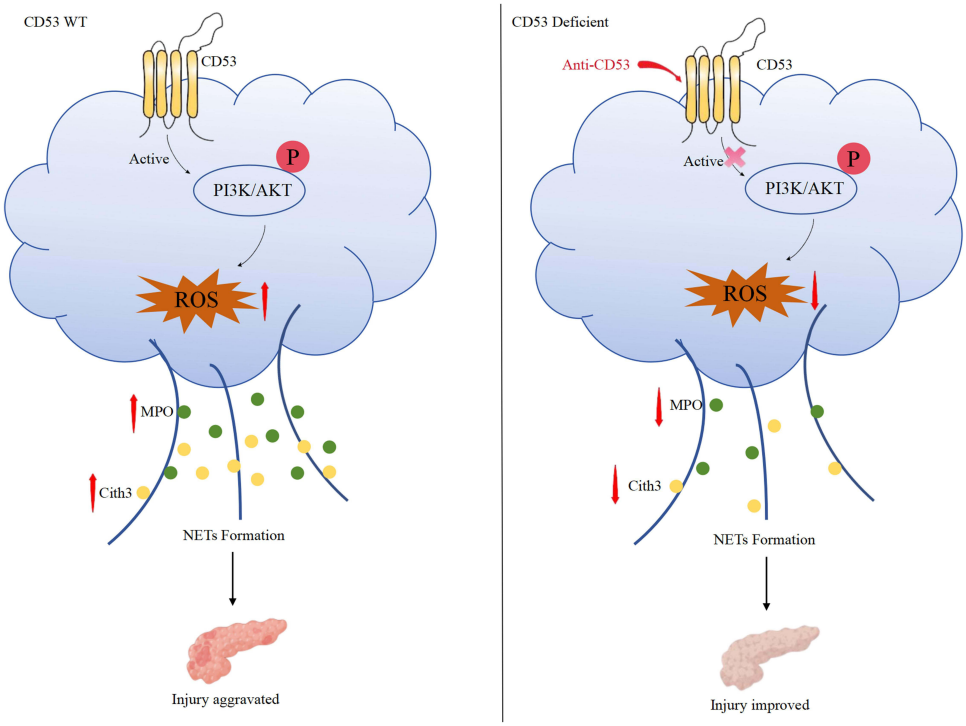

inflammatory reactions.[6] Therefore, identifying targets that modulate immune cell infiltration and the release of inflammatory mediators is crucial to attenuate the severity of AP.

Neutrophils are the primary effectors of acute inflammation and play a pivotal role in clearing extracellular pathogens.[7] During AP-induced pancreatic tissue damage, neutrophils are the first responders to migrate from circulation to the injured site, where they form neutrophil extracellular traps (NETs).[8] NETs significantly contribute to AP development, mediating inflammation and intensifying its severity.[9] The level of NETs formation was also positively correlated with the clinical prognosis of AP. Previous research by our group identified CD177 and gasdermin D as mediators of NET formation. Notably, the levels of peripheral neutrophil CD177 and gasdermin D in AP patients closely correlate with NETs levels and clinical prognosis.[10], [11] Targeting NETs formation and its key components can mitigate pancreatic tissue injury, inflammatory response in AP mice, and minimize distant organ damage.[12–14] Regrettably, current intervention lacks effective targets that can precisely address NETs formation to prevent and treat AP-related inflammatory injuries.

CD53,also known as MOX44 or TSPAN25, belongs to a novel tetraspanin family and is a pan-leukocyte antigen expressed across various white blood cells, including B cells, T cells, monocytes, and granulocytes.[15] CD53 serves critical roles in the immune system, playing parts in B-cell development, lymphocyte trafficking, and inflammatory and tumor diseases.[16–18] Recent studies demonstrate CD53's involvement in early B-cell development and lymphocyte recycling by stabilizing L-selectin on lymphocyte surfaces.[19,20] In addition, CD53 influences cell activation by inhibiting α3 integrin, thereby enhancing cell adhesion and promoting white blood cell aggregation at inflammatory sites.[21]

To date, it has not been reported whether CD53 promotes inflammation of AP through the release of NETs. Therefore, this study aims to explore the immunomodulatory role of CD53-mediated NETs formation in pancreatic necrosis and inflammatory injury of AP.

Materials and Methods

Animals

Male wild-type C57BL/6J mice, weighing approximately 20–25g, were procured from GemPharmatech Co.Ltd., Nanjing, China. The mice were housed in a standard pathogen-free room with a 12-hour light / 12-hour dark cycle, maintained at a temperature of 20–25°C. They were provided with standard rodent food and ad libitum access to water.

Patients

All patient samples were sourced from the Department of Gastroenterology, Affiliated Hospital of Yangzhou University, between October 2022 and October 2023. The study included a total of 61 AP patients and 20 healthy volunteers. Clinical characteristics of AP patients and healthy volunteers are detailed in Supplementary Table 1 and Supplementary Table 2.

AP diagnosis was based on the revised Atlanta Classification, 2012, requiring the presence of at least two of the following three criteria:[22] (1) Abdominal pain: acute, persistent, radiating to the back; (2) Serum lipase activity (or amylase activity) at least three times the upper limit of normal; (3) Radiological findings (USG/CT/MRI) indicating acute pancreatitis.[23] Exclusion criteria included: (1) age <18 or >80 years; (2) pregnancy period; (3) Previous history of tumors; (4) Recurrent pancreatitis; (5) Incomplete information. Patients were categorized into AP without multiple organ dysfunction syndrome (MODS) and AP with MODS groups based on the modified Marshall score system,[23] defining MODS as failure of two or more organs (cardiovascular, lung, kidney) for 48 hours or longer. Subgroups were also created based on the presence of local complications and systemic inflammatory response syndrome. AP patients were divided into AP without local complications (Non-LC-AP) and AP with local complications (LC-AP), AP without systemic inflammatory response syndrome (Non-SIRS-AP) and AP with systemic inflammatory response syndrome (SIRS-AP).

Processing of Human Peripheral Blood Samples

Blood samples of AP patients were collected using anticoagulant-containing collection vessels. Samples were mixed with sterile PBS solution in a 1:1 ratio. Lymphoprep (Alere Technologies AS, Oslo, Norway) was added to a 15mL centrifuge tube, followed by slow addition of the blood-PBS mixture along the tube wall. Centrifugation at a gradient of 800g for 20 minutes allowed for collection of cells in the lower layer. Neutrophils were isolated following red blood cell lysis.

Cell Culture

Mouse bone marrow-derived neutrophils: The femur and tibias of male C57BL/6J mice aged 6–8 weeks were isolated, muscle tissue was excised, the femur and tibia were placed in pre-cooled 1640 medium (BC-M-017, BIO-Channel). Both ends of the bones were trimmed, exposing the bone marrow cavity. The cavity was rinsed with 1640 medium, filtered using a 70μm cell filter (CLS431751, MERCK), and centrifuged at 450g for 10 minutes at room temperature. The supernatant was discarded, and neutrophils were isolated using the mouse peripheral blood neutrophil isolation kit (P9201, Solarbio), carefully collecting the neutrophilic layer fluid. After suspension dilution in 1640 medium, centrifugation was done at 4°C, 1200 rpm for 5 minutes. Following removal of the supernatant, cells were suspended in 1640 complete medium (90% 1640 + 10% FBS) and incubated in a 5% CO_2 cell incubator at 37°C for subsequent use.

Reagents and Antibodies

Details of all reagents and antibodies utilized in the study are provided in Supplementary Table 3 and Supplementary Table 4.

Acute Pancreatitis Model Preparation and Drug Intervention

For the Anti-CD53 (124701, BioLegend) intervention experiment, mice were divided into a caerulein-induced AP group (Cae) and various dose gradients of Anti-CD53 treatment group (Cae/Anti-CD53, 40μg/kg, 80μg/kg, 160μg/kg), along with a normal control group. The acute pancreatitis model was induced by intraperitoneal caerulein injections (100μg/kg at hourly intervals for 10 times) in the AP and Anti-CD53 groups. The normal control group received intraperitoneal

injections of the same volume of phosphate-buffered saline (PBS) as the other groups, while the AP group received an equivalent amount of IgG based on the maximum Anti-CD53 dose.

Sample Collection

The mice were anesthetized with Zoletil and euthanized 12 hours after the initial injection of caerulein. Blood samples were collected from the eye at 12 hours and analyzed for serum amylase and lipase levels following the kit instructions. Pancreatic tissue was extracted, fixed in 4% paraformaldehyde, and embedded in paraffin blocks for hematoxylin and eosin staining. Any remaining pancreatic tissue was preserved at −80°C.

Histological Analysis

Pancreatic tissue was fixed in 4% paraformaldehyde for 48 hours, embedded in paraffin blocks and sliced. The tissue sections were stained with hematoxylin eosin (H&E), dehydrated with gradient ethanol, transparent with xylene, sealed with neutral gum, and interpreted under an optical microscope. Histological scoring of pancreatic tissue was conducted by two independent pathologists in a blinded manner as previously described.[24]

Immunofluorescence Staining

Mouse pancreatic tissues were fixed, embedded, and sectioned. Sections were subjected to antigen retrieval by boiling in a sodium citrate buffer. The tissue sections were then blocked with normal goat serum, incubated overnight at 4°C with Anti-MPO (1:100, Abcam) and Anti-Cith3 (1:300, Abcam) or Anti-MPO (1:100, Abcam) and Anti-CD53 (1:100, Senta) in the dark. The next day, the slices were washed three times with PBS for three minutes each time. They were then incubated at room temperature for 2 hours with biotinized secondary antibody (1:1000 dilution). Finally, the tissue sections were incubated at room temperature in 4, 6-Diamino-2-phenylindole (DAPI) solution and sealed. After drying, the sample was observed using a confocal microscope (Leica TCS Sp8 sted, Germany), images were acquired and analyzed using its corresponding LAS X imaging software.

Measurement of NETs Related Indicators in vitro

Isolated mouse bone marrow neutrophils were seeded in 12-well plates and cultured in RPMI 1640 medium supplemented with 10% fetal bovine serum (FBS) at 37°C and 5% CO_2 for 30 minutes. In vitro NETs model was constructed by treating 100 nM PMA or PBS for 4 hours. The formation of NETs in vitro was visualized by immunofluorescence. The cells were fixed with 4% paraformaldehyde, washed with PBS, incubated with Anti-MPO (1:100, Abcam) and Anti-Cith3 (1:300, Abcam) at 4°C overnight, stained with a biotinylated secondary antibody, and counterstained with DAPI. The samples were then examined under a confocal microscope (Leica TCS Sp8 sted, Germany) and analyzed using LAS X imaging software.

Elisa

Cell supernatants and serum from experimental animals were collected. 96-well plates were coated with specific antibodies and incubated for 12 hours. The levels of TNF-α (88–7324-77, Affymetrix Ebioscience), MCP-1 (88–7391-77, Affymetrix Ebioscience), and IL-6 (88–7064-77, Affymetrix Ebioscience) were determined following the kit instructions.

Flow Cytometry

MPO determination: The treated mouse bone marrow neutrophils were exposed to surface antibodies (Anti-CD45.2, Anti-CD11b and Anti-Ly6G) at 4°C for 30 minutes, washed with PBS, fixed with fixative at 4°C for 20 minutes, and then washed with PBS. Anti-MPO antibody was stained at 4°C for 20 minutes. After washing with PBS, the cells were suspended with 200μL PBS. Finally, we collected cells at Beckman DxFlex B5-R3-V3 (Indianapolis, IN, United States), CytExpert for DxFlex was used for analysis.

ROS determination: DHE fluorescent probe (Sigma, D70N8, 1:2000) was used to detect the content of intracellular reactive oxygen species.[12] The treated mouse bone marrow neutrophils were incubated with DHE solution at 37°C for

30 minutes without light. The cells were washed with PBS and then stained with surface antibodies (Anti-CD45.2, Anti-CD11b, and Anti-Ly6G) at 4°C for 30 minutes. After washing the cells with PBS, the cells were suspended with 200μL PBS. Finally, cells were collected as above for analysis.

$CD53^+$ neutrophils determination:The extracted human peripheral blood neutrophils were stained with surface antibodies (Anti-CD45, Anti-CD11b, Anti-CD66b, and Anti-CD53) at 4°C for 30 minutes. After washing the cells with PBS, the cells were re-suspended with 200μL PBS. Finally, the cells were collected and analyzed as above.

RNA Sequencing and Bioinformatics Research Methods

mRNA expression profiles pre and post PMA-induced NETs formation were analyzed using RNA-seq technique. Total RNA from the control and PMA-treated groups was extracted using TRNzol universal reagent (TIANGEN, China) and processed for RNA-seq by Novogene (Tianjin, China). Differential gene expression analysis was conducted using volcano plot and heatmap analysis in R software to identify differentially expressed genes (DEGs) between the two groups. To identify differentially expressed genes (DEGs), we used the "DESeq2" software package with adjusted p-value < 0.05 and |log2FC| >1.[25] We used online tools (https://www.bioinformatics.com.cn/static/others/jvenn/example.html) to draw Venn diagrams. The R packages "Enhanced Volcano" and "pheatmap" were used to visualize the differential expression and clustering of genes in the sequencing dataset.

Furthermore, mRNA expression in PMA group and PMA+Anti-CD53 group was assessed using RNA-seq. Total RNA from these groups was isolated using Trzol universal reagent (TIANGEN, China) and then subjected to RNA-seq by Novogene Company (Tianjin, China). Subsequently, KEGG enrichment analysis[26] was performed to using R software uncover gene pathway associations.

Protein Extraction and Western Blot Analysis

Cells were lysed using ultrasonic homogenization, and the resulting supernatant was collected by centrifugation (12,000 rpm, 30 minutes). Protein concentration was determined using a BCA protein kit (P0012, Beyotime). The remaining supernatants were added with 5X protein loading buffer (P0015, Beyotime), denatured at 100°C for 10 minutes, and stored at −80°C.

The protein samples underwent 10% SDS-polyacrylamide gel electrophoresis (PAGE), followed by transfer onto a PVDF membrane and blocking with 5% skim milk at room temperature for 2 hours. The membrane was then probed with primary antibodies, including Anti-PAD4 (1:1000, Abcam), PI3 Kinase p85 (19H8) Rabbit mAb (1:1000, CST), Phospho-PI3 Kinase p85 (Tyr458)/p55 (Tyr199) (E3U1H) Rabbit mAb (1:1000, CST), Akt (pan) (C67E7) Rabbit mAb (1:1000, CST), Phospho-Ak t (Ser473) (D9E) Rabbit mAb (1:1000, CST) and Anti-β-actin (1:1000, CST) at 4°C overnight. On the second day, use TBST washing film 3 times for 15 minutes each time. The membrane was then incubated with the second antibody coupled with horseradish peroxidase at 37°C for 2 hours. Finally, use TBST washing film 3 times, each time for 15 minutes. After washing, protein bands were detected using the ECL Plus chemiluminescence system. Image intensity was analyzed using ImageJ software.

Scanning Electron Microscope (SEM) Observation

The sample underwent fixation at 4°C for 24 hours with 2.5% glutaraldehyde, followed by standard dehydration, critical point drying, heavy metal sputter coating, and enhancement of electrical conductivity. Subsequently, the morphology of NETs was visualized using a scanning electron microscope (GeminiSEM 300, UK).

Statistical Analysis

Statistical analysis was performed using GraphPad Prism 9.0, R Project, SPSS and Mengte Cloud Statistical Platform. A Student's *t*-test was utilized for comparison of means between two groups, while one-way analysis of variance (ANOVA) was employed to assess statistical differences between multiple groups. Results are presented as mean ± standard error (SE), and histogram data is expressed as mean ± standard error of the mean (SEM). A significance level of $P < 0.05$ indicates a two-tailed difference. Each experiment was replicated three times for robustness.

Results

CD53 Is Significantly Highly Expressed in PMA-Induced NETs and AP Mice

In the PMA-induced NETs formation model, the RNA of mouse bone marrow neutrophils pre and post PMA induction was extracted for RNA sequencing analysis. To reduce batch differences, we jointly analyzed the two batches of NETs model RNA-Seq database of our research group and found that a total of 16,118 differential genes overlapped in the two sets of data, and further analysis revealed significant changes in various cell surface molecules. We combined the change of P-value and Log2FoldChange, and finally screened through volcanic map and heat map analysis and found that CD53 significantly increased after PMA-induced NETs formation (Figure 1A-B). In order to further verify the changes in CD53 expression during the formation of NETs, WB, flow cytometry and RT-PCR experiments were respectively used to verify the significantly high expression of CD53 in NETs (Figure 1C-F).

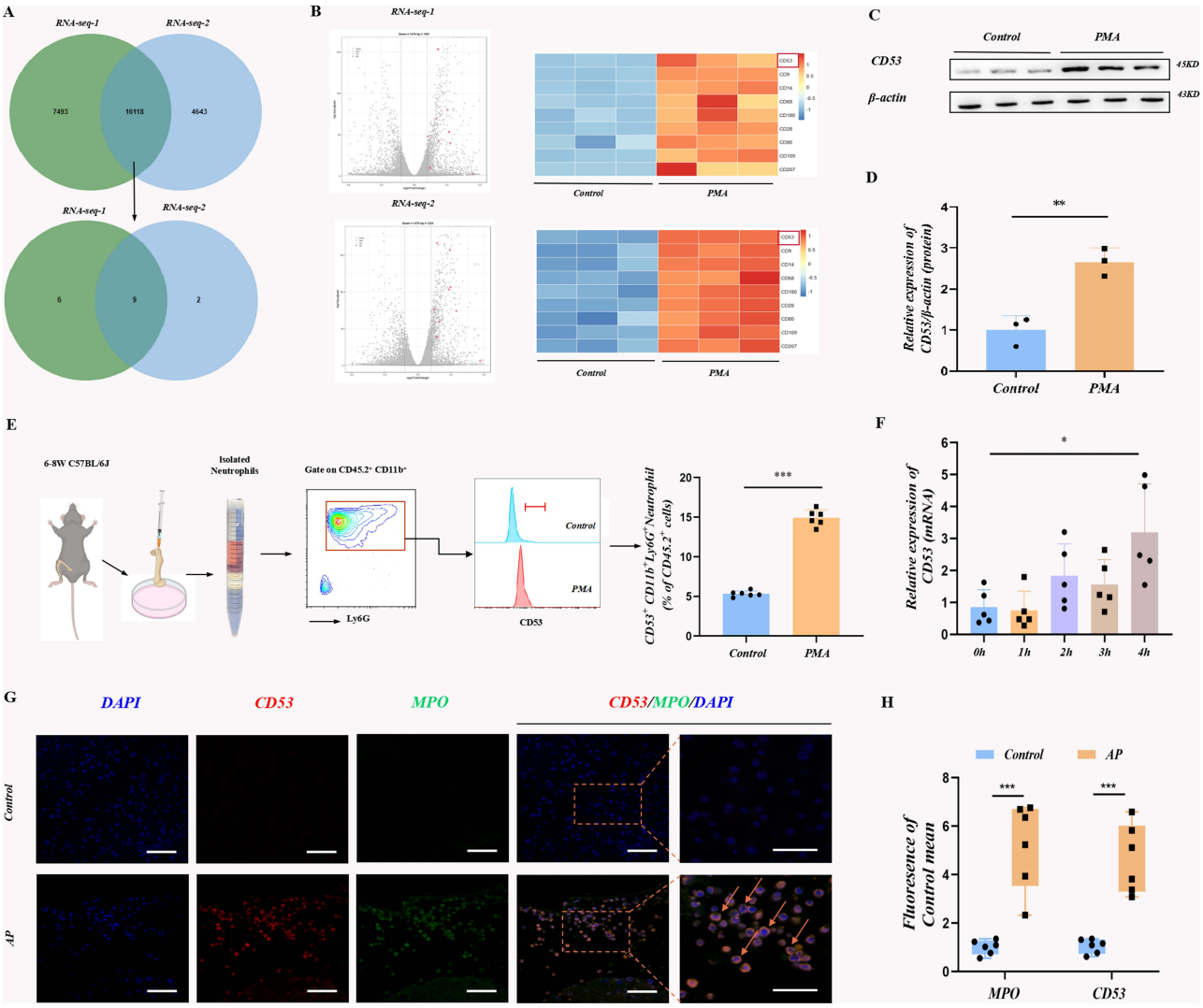

Figure 1 CD53 is significantly highly expressed in PMA-induced NETs and AP mice. (**A**) Flow chart of combined analysis of two sets of transcriptome sequencing data cultured from bone marrow neutrophils isolated from C57BL/6J male mice aged 6 to 8 weeks and stimulated with PMA (100 nM) for 4 hours. (**B**) Overlapping of the two sets of data for differential surface molecular volcano maps and heat map analysis. (**C-D**) Western blotting was used to analyze the protein levels of CD53 in neutrophils and the corresponding semi-quantitative analysis (N=3 per group). β-actin is used as a control for proteins. (**E**) Mouse bone marrow derived neutrophils were stimulated with PMA (100 nM) for 4 hours and then stained for flow cytometry analysis. Representative flow cytometry of C57BL/6 J mouse bone marrow neutrophils ($CD45.2^+CD11b^+Ly6G^+$). Representative flow cytometry and bar charts describing neutrophil proportions and CD53 expression levels. Data are expressed as mean ± SE (N=6 per group). (**F**) Mouse bone marrow derived neutrophils were stimulated with PMA (100 nM) at different time gradients to analyze CD53 mRNA levels by RT-PCR. (**G**) The AP mouse model was induced by caerulein, and the mouse pancreatic tissue was stained with CD53 and MPO immunofluorescence, the scale = 50μM. (**H**) Optical density analysis of CitH3 and MPO fluorescence (N=6 per group). Statistical significance was indicated by *P<0.05,** P<0.01,***P<0.001.

Moreover, the AP mouse model was also induced by caerulein. Immunofluorescence detection results showed that CD53 and MPO co-localization in damaged pancreatic tissue of AP group was significantly higher than that of control group, suggesting that CD53 was mainly highly expressed in neutrophils after AP (Figure 1G-H). These findings suggest a significant overexpression of CD53 in both NETs formation and AP mice in vitro.

CD53 is Highly Expressed in Peripheral Blood Neutrophils of AP Patients and is Closely Related to Disease Severity

61 AP patients were included in the study, peripheral blood samples were collected for analysis. The clinical characteristics of AP patients are shown in Supplementary Table 1. Peripheral blood neutrophils from AP patients and healthy controls were analyzed by flow cytometry. As shown in Figure 2A, polymorphonuclear leukocytes (PMN) and $CD53^{+}$PMN were significantly increased in AP patients compared to Control. AP patients were divided into AP non-MODs (N=47) and AP with MODS (MODS AP) groups (N=14) according to the modified Marshall score. According to the occurrence of local complications or systemic inflammation, AP patients were divided into two groups: Non-LC group (N=39) and LC group (N=22), Non-SIRS group (N=40) and SIRS group (N=21). We found that the expression level of peripheral neutrophils CD53 in AP patients with poor prognosis was significantly higher than that in the control group, and was correlated with the severity of the disease (Figure 2B-D).Correlation heat map analysis demonstrated a positive correlation between peripheral neutrophil CD53 levels and serum C-reactive protein,White Blood Cell, and other indicators (R=0.43, P=0.0002) (Figure 2E). In addition, ROC curve analysis showed that the area under the curve of $CD53^{+}$PMN(%) was 0.83 ($P < 0.001$, Sensitivity 76.92%, Specificity 86.33%) (Figure 2F). We found that $CD53^{+}$PMN was more accurate and sensitive than PMN and CRP in predicting progression to MODS in AP patients.

To further analyze the changes of NETs in patients with acute pancreatitis. We used flow cytometry to analyze NETs-related indicators (MPO) in healthy controls and AP, and the expression of NETs-related indicators (MPO) and CD53 was significantly increased in AP patients compared with controls, and the two were positively correlated (Supplementary Figure 1). In summary, CD53 was significantly overexpressed in AP patients and correlated with disease severity.

Anti-CD53 Significantly Reduces PMA-Induced NETs Formation

In Figure 3A, different concentrations of Anti-CD53 (10, 20, and 40 ng/mL) were assessed for MPO and ROS production in mouse bone marrow neutrophils post PMA stimulation using flow cytometry. MPO and ROS are important substances for the early formation of NETs.[27] Significant protection against MPO and ROS was observed in the Anti-CD53 40 ng/mL group compared to other doses. Subsequently, immunofluorescence and scanning electron microscopy confirmed (Figure 3B-C) that PMA-induced neutrophils formed extensive NETs structures, which were significantly inhibited by treatment with Anti-CD53. In addition, Pro-inflammatory cytokine levels in PMA-induced neutrophil supernatant were also inhibited by Anti-CD53 (Figure 3D). As shown in Figure 3E-F, WB confirmed that the expression of PAD4, a key enzyme involved in NETs production,[28] was also significantly reduced after treatment with Anti-CD53.

Anti-CD53 Inhibits the Formation of NETs Through the PI3K/AKT Signaling Pathway

To elucidate the mechanism of CD53 in the formation of NETs, we extracted RNA from mouse bone marrow derived neutrophils in the PMA group and the PMA+Anti-CD53 group for RNA-Seq (Figure 4A). PCA analysis was performed on the sequencing data of PMA group and PMA+Anti-CD53 group (Figure 4B). The differences between the PMA group and the PMA+Anti-CD53 group are reflected in the volcano map (Figure 4C). KEGG enrichment analysis showed significant changes in the PI3K/AKT signaling pathway (Figure 4D). Previous studies have shown that the PI3K/AKT signaling pathway can activate NADPH enzyme, thereby mediating the production of ROS and promoting the formation of NETs, which is one of the key pathways in the formation of NETs.[29] Subsequently, we examined the effect of CD53 on the PI3K/AKT pathway. As shown in Figure 4E, we found that the expression of P-PI3K and P-AKT protein in neutrophils in the PMA group was increased, but the expression of P-PI3K and P-AKT protein was significantly decreased after Anti-CD53 administration (Figure 4F). Subsequently, we sought to verify whether Anti-CD53 inhibited

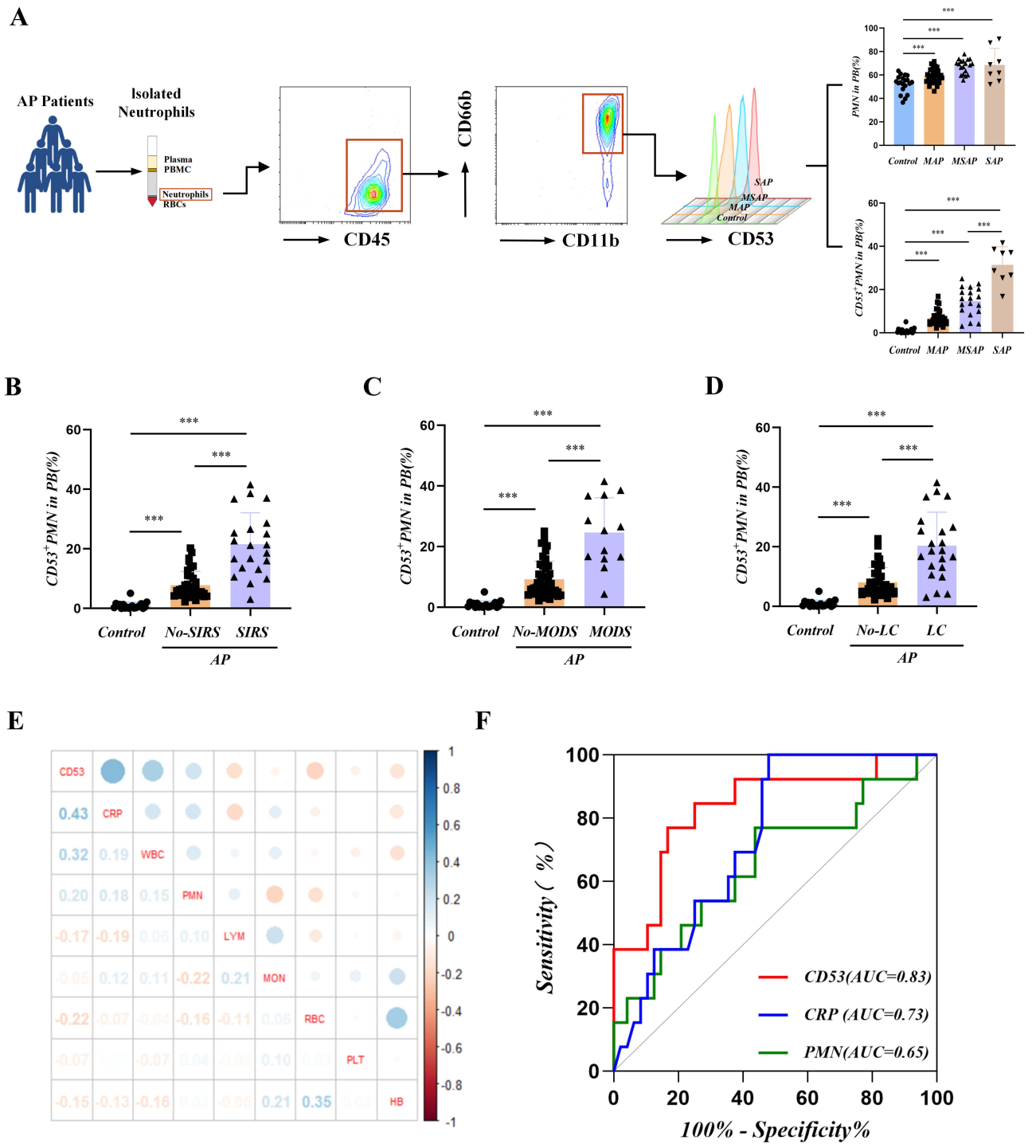

Figure 2 CD53 is highly expressed in peripheral blood neutrophils of AP patients and is closely related to disease severity. (**A**) Flow cytometry gated ($CD45^+CD11b^+CD16^+$) of a representative sample of human peripheral blood neutrophils, with representative flow cytometry graphs and bar plots depicting CD53 expression levels in neutrophils. Data are expressed as mean ±SE. (**B**) Percentage of $CD53^+$ neutrophils ($CD45^+CD11b^+CD16^+$) in peripheral blood in control, Non-SIRS and SIRS groups. (**C**) Percentage of $CD53^+$ neutrophils ($CD45^+CD11b^+CD16^+$) in peripheral blood in control, Non-MODS, and MODS groups. (**D**) Percentage of $CD53^+$ neutrophils ($CD45^+CD11b^+CD16^+$) in peripheral blood in control group, Non-LC group and LC group. (**E**) Heat maps of correlations between neutrophil CD53 levels and other clinical indicators in AP patients. (**F**) Diagnostic value of $CD53^+$PMN, PMN, CRP level ROC curve analysis for MODS. Statistical significance was indicated by ***P<0.001.

the formation of NETs only through the PI3K/AKT signaling pathway. In Figure 4G, flow cytometry was used to assess MPO and ROS production in mouse bone marrow neutrophils after PMA stimulation with different concentrations of LY094002 (1, 10, and 100 μM). LY094002 is a PI3K/AKT pathway inhibitor. Compared with other doses, LY094002

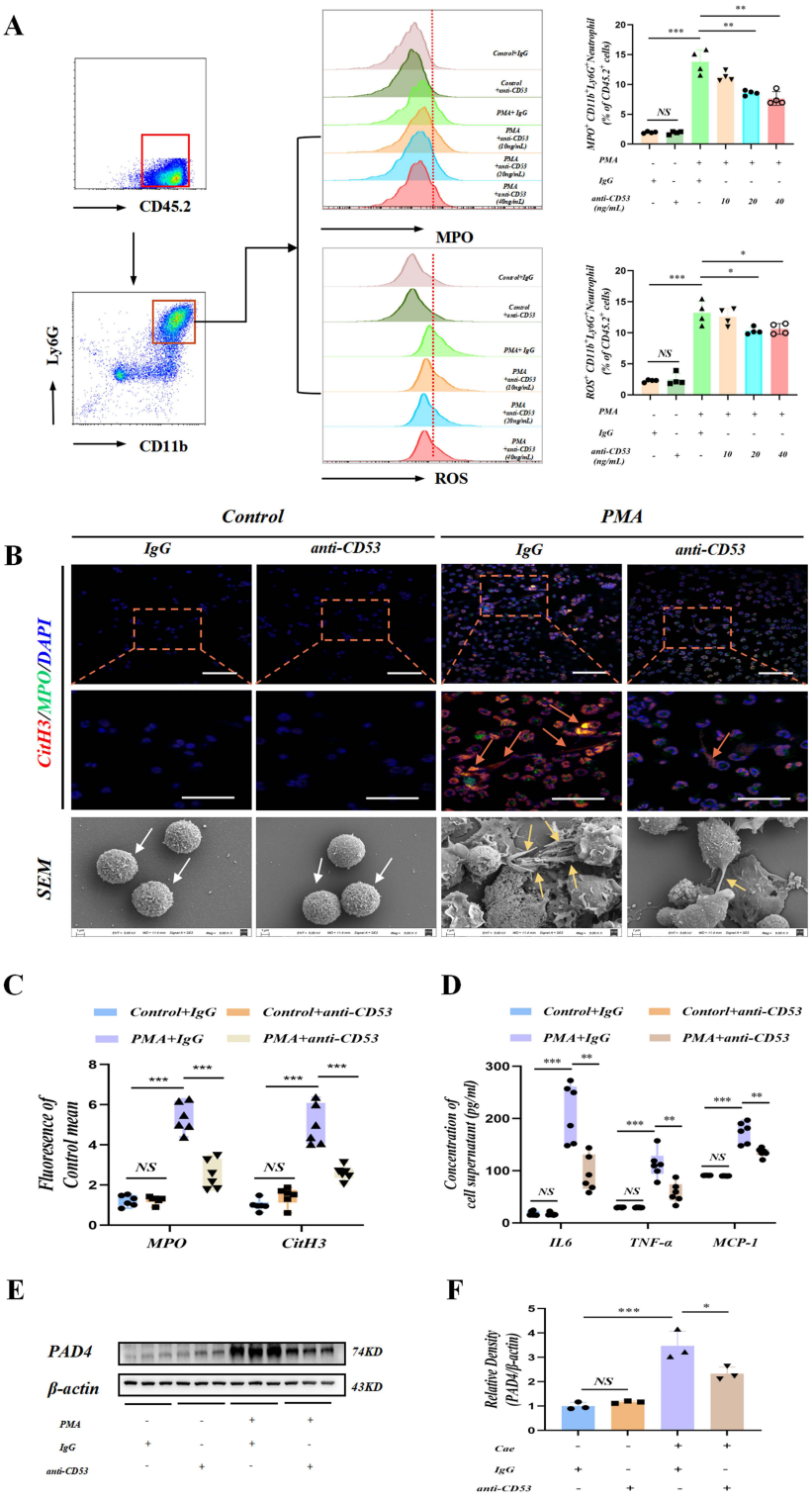

Figure 3 Inhibition of CD53 significantly reduces NETs formation in vitro. (**A**) Bone marrow neutrophils isolated from C57BL/6J male mice aged 6 to 8 weeks were cultured with PMA (100 nM), incubated with different doses of Anti-CD53 (10, 20, and 40 ng/mL), and then stained for flow cytometry analysis. Representative flow cytometry of C57BL/6 J mouse bone marrow neutrophils ($CD45.2^+$ $CD11b^+$ $Ly6G^+$). Representative flow cytometry and bar charts describing neutrophil proportions and MPO and ROS expression levels. Data are expressed as mean ± SE (N=4 per group). (**B**) Representative immunofluorescence images of CitH3 and MPO at 400X and 1000X magnifications (N=6 per group). Scale=50μM. Representative SEM images of neutrophils at 5000X magnification (N=6 per group). Scale = 1μM. Red arrows represent NETs under immunofluorescence, white arrows represent normal neutrophils, and yellow arrows represent NETs under SEM. (**C**) Optical density analysis of CitH3 and MPO fluorescence (N=6 per group). (**D**) The levels of IL-6, TNF-α and MCP-1 were determined by ELISA (N=6 per group). (**E-F**) The protein level of PAD4 in neutrophils (N=3 per group) and the relative protein expression histogram of PAD4 were analyzed by Western blot. β-actin is used as a control for proteins. Statistical significance was indicated by *P<0.05,** P<0.01,***P<0.001. No significance was indicated by 'NS'.

https://doi.org/10.2147/JIR.S507886

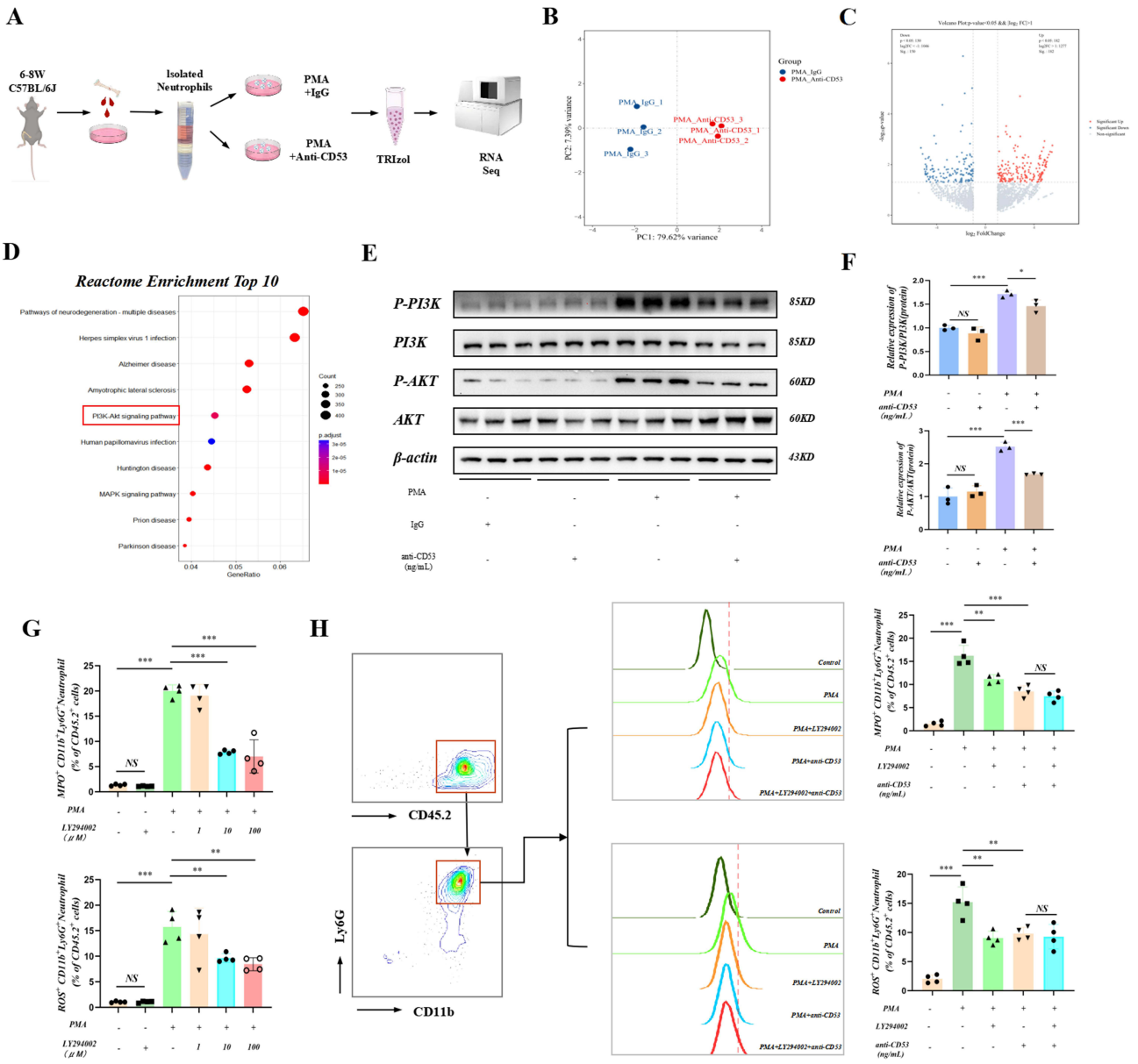

Figure 4 Anti-CD53 inhibits the formation of NETs via the PI3K/AKT signaling pathway. (**A**)RNA was extracted from mouse bone marrow derived neutrophils in PMA group and PMA+Anti-CD53 group for RNA-seq. (**B**) PCA analysis of sequencing data. (**C**) Volcanic map analysis of differential genes. (**D**) Differential gene response group enrichment analysis of PMA group and PMA+Anti-CD53 group (N=3 per group). (**E**) The expression levels of P-PI3K and P-AKT in neutrophils were detected by Western method. (**F**) The relative protein expression of P-PI3K and P-AKT in neutrophils, with PI3K and AKT as the protein load control (N=3 per group). (**G-H**) Representative flow cytometry of C57BL/6 J mouse bone marrow neutrophils ($CD45.2^+$ $CD11b^+$ $Ly6G^+$). Representative flow cytometry and bar charts describing neutrophil proportions and MPO and ROS expression levels. Data are expressed as mean ± SE (N=4 per group). Statistical significance was indicated by *P<0.05,** P<0.01,***P<0.001. No significance was indicated by 'NS'.

100 μM group had a significant protective effect on MPO and ROS. Proceed to the next step, the addition of Anti-CD53 did not further improve the formation of NETs during LY094002 treatment (Figure 4H). These results support the conclusion that CD53 inhibits the formation of NETs through the PI3K/AKT signaling pathway.

Anti-CD53 Efficacy in Reducing Pancreatic Injury in AP Mice

Based on the prior dose-response experiment (Supplementary Figure 2), a dose of 160μg/kg Anti-CD53 was validated in subsequent experiments. As shown in Figure 5A, Anti-CD53 intervention significantly alleviated pancreatic tissue edema, inflammatory cell infiltration and acinar cell necrosis in mice, and also significantly reduced serum amylase and lipase levels and inflammatory factors (Figure 5B and Figure 5DFigure 5E). In addition, immunofluorescence detection showed that the formation of NETs (Cith3/MPO colocalization) in pancreatic tissue of mice treated with Anti-CD53 was significantly reduced compared with the control group (Figure 5A and Figure 5C). These findings suggest the efficacy of Anti-CD53 in protecting against pancreatic injury, reducing inflammation, and inhibiting NETs formation in the pancreatic tissue of AP mice.

Discussion

This study provides new insights that inhibition of CD53 can reduce the formation of NETs and protect against inflammatory injury in AP through the PI3K/AKT pathway. These findings elucidate the mechanism of CD53 in NETs formation and highlight that CD53 is a key factor in AP-targeting inflammatory injury.

Studies have shown that neutrophils rapidly infiltrate pancreatic tissue during the early inflammatory response, forming NETs that contribute to the inflammatory process.[30] Activated neutrophils form NETs that participate in the inflammatory process.[31] Excessive release of NETs may have proinflammatory effects,[32] then aggravated acute pancreatitis. To investigate further, we recruited 61 AP patients and 20 healthy controls, revealing significantly elevated CD53, WBC, and CRP levels in the serum of AP patients, correlating with disease severity. Subsequently, in a mouse AP model, Anti-CD53 intervention significantly reduced pancreatic injury and inflammatory infiltration, offering strong support for targeting CD53 as a potential therapeutic approach in AP. Next, we established a mouse AP model and applied Anti-CD53 intervention, and the results proved that Anti-CD53 could significantly reduce pancreatic injury and inflammatory infiltration of AP. Taken together, these results strongly support the potential therapeutic effect of targeting CD53 in AP.

Recent research has highlighted that the four-transmembrane protein CD53, which is widely expressed in immune cells and positively correlated with the level of immune cell infiltration,[33] plays a crucial role in cellular immune responses.[15,34] CD53 has a variety of roles in immune cells, such as response to pathogens, adhesion, migration[21] and signaling.[35] The co-localization of CD53 and MPO confirmed the regulatory role of CD53 in neutrophil-forming NETs, so we focused on the role of CD53 in NETs. The data presented here extend previous literature showing that neutrophil CD53, but not lymphocyte CD53, mediates inflammatory responses. Existing reports have demonstrated a multifunctional role for CD53 in different cell types and processes.[16,36,37] Future studies will better distinguish the relative contribution of CD53 from different cell sources to the body's inflammatory response. Understanding these data in the light of the previous literature on CD53 function raises interesting points for further investigation, particularly regarding the relationship between CD53 and neutrophils. Beinert et al proposed that the expression of CD53 is increased in senescent neutrophils,[38] Neutrophils have traditionally been considered short-acting effector cells in the innate immune system with a half-life of about 19 hours.[39] Our methodologic observation window was 4 hours, well before the accepted half-life of aging, and our experiments were rigorously controlled. Thus our findings do not conflict with the conclusions of Beinert et al. Previous studies by Mollinedo et al found[40] that when neutrophils were stimulated by PMA, the expression level of CD53 was reduced. This conclusion seems inconsistent with our results, and we consider that several factors may have contributed to this difference: first, the specific timing of PMA processing is different, different methodologies may lead to neutrophils displaying different cell biological functions in different states. Second, our study is focused on discussing the expression levels of CD53 in NETs, which have been shown to be released by most neutrophils upon death 2–4 hours after activation.[41,42] Finally, we also verified that the expression of CD53 in NETs was up-regulated by RNA sequencing, flow cytometry, WB, and PCR. Through a series of in vitro and in vivo experiments, we verified that Anti-CD53 effectively inhibits NETs formation in AP, and reducing inflammatory cytokine levels such as IL-6, TNF-α, and MCP-1. The regulatory effect of CD53 on NETs formation via neutrophils was confirmed by CD53 and MPO colocalization.

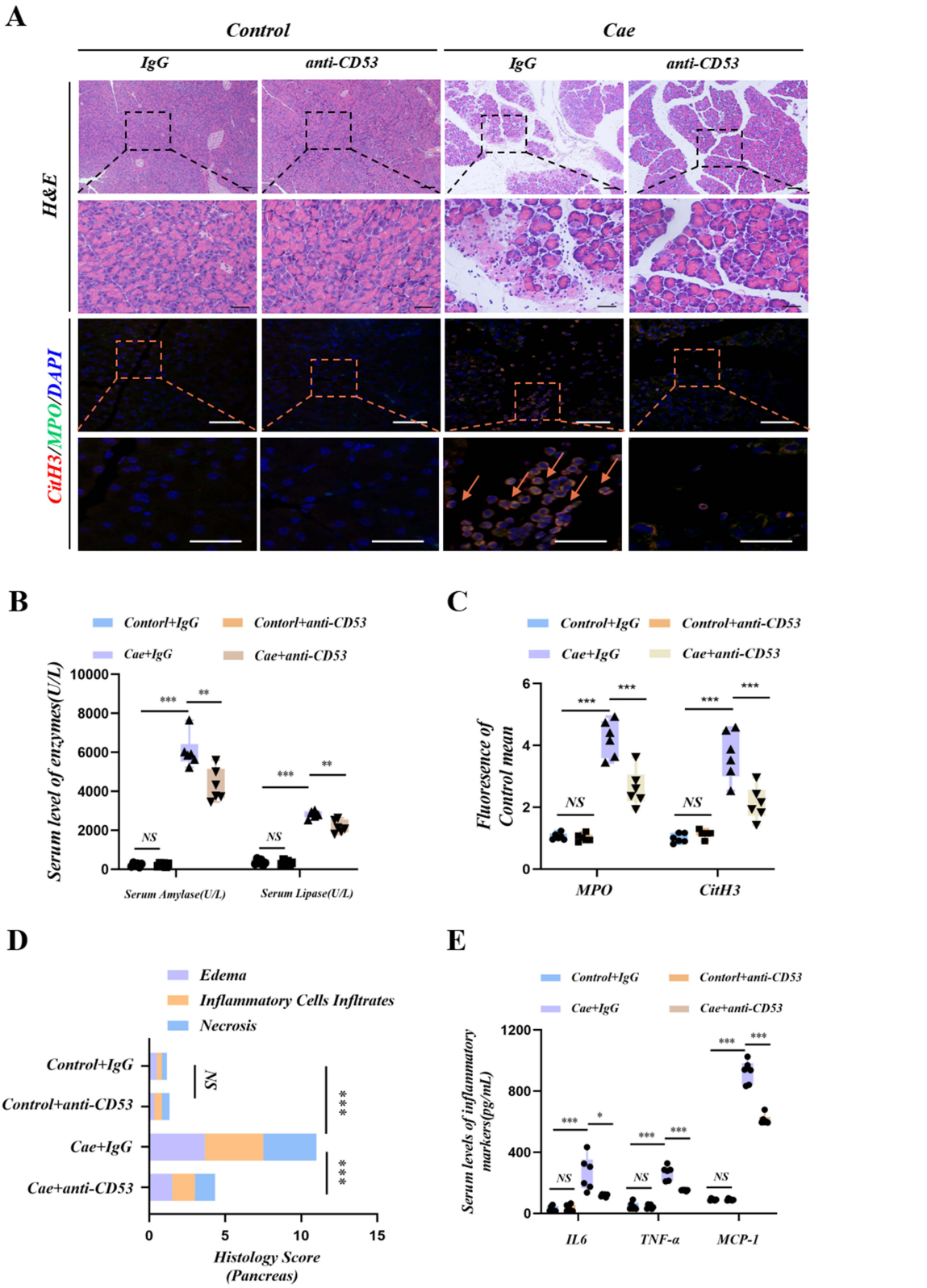

Figure 5 Anti-CD53 significantly alleviates pancreatic injury in AP mice. (**A**) Representative HE staining of pancreatic tissue at 100X and 400X magnifications. Scale=50μM. Representative immunofluorescence images of CitH3 and MPO of pancreatic tissue at 400X and 1000X magnifications (N=6 per group). Scale=50μM. Red arrows represent NETs under immunofluorescence. (**B**) Serum amylase and lipase levels. (**C**) Optical density analysis of MPO and CitH3 fluorescence (N=6 per group). (**D**) Pathological scores of pancreatic tissue (N=6 per group). (**E**) Serum IL-6,TNF-α and MCP-1 levels were measured by ELISA (N=6 per group). Statistical significance was indicated by *P<0.05,** P<0.01,***P<0.001. No significance was indicated by 'NS'.

In addition, the PI3K/AKT pathway in myeloid immune cells is implicated in regulating immune cell activation by modulating anti-inflammatory cytokines and pro-inflammatory cytokines.[43] Guo.G et al demonstrated that DNase-I@V2C shifts neutrophil function from NETs to phagocytosis by activating the PI3K/AKT pathway in the diabetic microenvironment, thereby eliminating biofilm infections.[44] Zhu.C.L et al verified that NETs are overreleased during ARDS and that knocking down PD-L1 can inhibit the release of NETs through the PI3K/AKT pathway.[45] In this study, through RNA-Seq and subsequent functional validation, we found that CD53 promotes the formation of NETs through the PI3K/AKT pathway. Targeted inhibition of CD53 may inhibit the formation of NETs through PI3K/AKT signaling.

Conclusion

In conclusion, our findings represent the initial confirmation that CD53 triggers the PI3K/AKT pathway and fosters the formation of NETs formation. By modulating CD53, the generation of NETs can be thwarted, consequently mitigating inflammatory injury in AP mice. This study contributes to the understanding of NETs formation mechanisms and introduces innovative therapeutic approaches for managing AP and other inflammatory conditions associated with NETs.

Abbreviation

AP, Acute pancreatitis; CitH3, Citrullinated histone H3; CRP, C-reactive protein; ELISA, Enzyme-linked immunosorbent assay; KEGG, Kyoto Encyclopedia of Genes and Genomes; LC, Local complications; MPO, Myeloperoxidase; MODS, Multiple organ dysfunction syndrome; NETs, Neutrophil extracellular traps; PMA, Phorbol-12-myristate-13-acetate; PCA, Principal Component Analysis; RT-PCR, Reverse Transcription-Polymerase Chain Reaction; SIRS, Systemic inflammatory response syndrome; ROS, Reactive oxygen species; RNA-seq, RNA sequencing; SEM, Scanning Electron Microscope; SAP, Severe acute pancreatitis; WBC, White Blood Cell.

Data Sharing Statement

The data shown in this article are available from the corresponding authors upon a reasonable request.

Ethics Approval and Informed Consent

The patient samples were studied in accordance with the Declaration of Helsinki and approved by the Human Ethics Committee of the Affiliated Hospital of Yangzhou University [approval No. 2018-YKL11-27]. All patients were aware of and provided written informed consent. All animal procedures were conducted in accordance with the ethical policies and procedures approved by the ethics committee of Yangzhou University, China [approval No. 202211006].

Acknowledgments

All authors made a significant contribution to the work reported, whether that is in the conception, study design, execution, acquisition of data, analysis and interpretation, or in all these areas; took part in drafting, revising or critically reviewing the article; gave final approval of the version to be published; have agreed on the journal to which the article has been submitted; and agree to be accountable for all aspects of the work.

Funding

The project was supported by the National Natural Science Foundation of China [No.82400763;82241043], Natural Science Foundation of Jiangsu Province (No. BK20240500); Natural Science Foundation of Yangzhou [No. YZ2024186], National Natural Science Foundation of Shandong Province [RHB, No.ZR2021MH032], Yangzhou Key Laboratory of Pancreatic Diseases [No. YZ2021147] and Suzhou Innovation Platform Construction Projects-Municipal Key Laboratory Construction [No. SZS2023001].

Disclosure

The authors state that they have no known competing financial interests or personal relationships.

References

1. Zhang C, Li G, Lu T. et al. The interaction of microbiome and pancreas in acute pancreatitis. *Biomolecules*. 2023;14(1):59. doi:10.3390/biom14010059
2. Zhu Q. *The TRIM28/miR133a/CD47 Axis Acts as a Potential Therapeutic Target in Pancreatic Necrosis by Impairing Efferocytosis*; 2024; Mol Ther.
3. Yang ZW, Meng XX, Xu P. Central role of neutrophil in the pathogenesis of severe acute pancreatitis. *J Cell Mol Med*. 2015;19(11):2513–2520. doi:10.1111/jcmm.12639
4. Zhu Q, Yuan C, Dong X, et al. Bile acid metabolomics identifies chenodeoxycholic acid as a therapeutic agent for pancreatic necrosis. *Cell Rep Med*. 2023;4(12):101304. doi:10.1016/j.xcrm.2023.101304
5. Lee PJ, Papachristou GI, Speake C, et al. Immune markers of severe acute pancreatitis. *Curr Opin Gastroenterol*. 2024;40(5):389–395. doi:10.1097/MOG.0000000000001053
6. Glaubitz J, Asgarbeik S, Lange R, et al. Immune response mechanisms in acute and chronic pancreatitis: strategies for therapeutic intervention. *Front Immunol*. 2023;14:1279539. doi:10.3389/fimmu.2023.1279539
7. Liew PX, Kubes P. The neutrophil's role during health and disease. *Physiol Rev*. 2019;99(2):1223–1248.
8. Zhou X, Jin S, Pan J, et al. Damage associated molecular patterns and neutrophil extracellular traps in acute pancreatitis. *Front Cell Infect Microbiol*. 2022;12:927193.
9. Li H, Zhao L, Wang Y, Zhang MC, Qiao C,et al. Roles, detection, and visualization of neutrophil extracellular traps in acute pancreatitis. *Front Immunol*. 2022;13:974821.
10. Han F, Chen H, Chen L, et al. Inhibition of Gasdermin D blocks the formation of NETs and protects acute pancreatitis in mice. *Biochem Biophys Res Commun*. 2023;654:26–33. doi:10.1016/j.bbrc.2023.02.082
11. Zhang J, Yang X, Xu X, et al. CD177 inhibits neutrophil extracellular trap formation and protects against acute pancreatitis in mice. *J Clin Med*. 2023;12(7):2533.
12. Han F, Ding Z-F, Shi X-L, et al. Irisin inhibits neutrophil extracellular traps formation and protects against acute pancreatitis in mice. *Redox Biol*. 2023;64:102787. doi:10.1016/j.redox.2023.102787
13. Xu Q, Shi M, Ding L, et al. High expression of P-selectin induces neutrophil extracellular traps via the PSGL-1/Syk/Ca(2+)/PAD4 pathway to exacerbate acute pancreatitis. *Front Immunol*. 2023;14:1265344. doi:10.3389/fimmu.2023.1265344
14. Linders J, Madhi R, Rahman M, et al. Extracellular cold-inducible RNA-binding protein regulates neutrophil extracellular trap formation and tissue damage in acute pancreatitis. *Lab Invest*. 2020;100(12):1618–1630. doi:10.1038/s41374-020-0469-5
15. Dunlock VE. Tetraspanin CD53: an overlooked regulator of immune cell function. *Med Microbiol Immunol*. 2020;209(4):545–552. doi:10.1007/s00430-020-00677-z
16. Greenberg ZJ, Monlish DA, Bartnett RL, et al. The Tetraspanin CD53 regulates early B cell development by promoting IL-7R signaling. *J Immunol*. 2020;204(1):58–67. doi:10.4049/jimmunol.1900539
17. Månsson R, Lagergren A, Hansson F, et al. The CD53 and CEACAM-1 genes are genetic targets for early B cell factor. *Eur J Immunol*. 2007;37(5):1365–1376. doi:10.1002/eji.200636642
18. Bai M, Pan Q, Sun C. Tumor purity coexpressed genes related to immune microenvironment and clinical outcomes of lung adenocarcinoma. *J Oncol*. 2021;2021:9548648. doi:10.1155/2021/9548648
19. Yeung L, Gottschalk TA, Hall P, et al. Tetraspanin CD53 modulates lymphocyte trafficking but not systemic autoimmunity in Lyn-deficient mice. *Immunol Cell Biol*. 2021;99(10):1053–1066. doi:10.1111/imcb.12501
20. Sabat R, Šimaitė D, Gudjonsson JE, et al. Neutrophilic granulocyte-derived B-cell activating factor supports B cells in skin lesions in hidradenitis suppurativa. *J Allergy Clin Immunol*. 2023;151(4):1015–1026. doi:10.1016/j.jaci.2022.10.034
21. Yeung L, Anderson JML, Wee JL, et al. Leukocyte Tetraspanin CD53 restrains α(3) integrin mobilization and facilitates cytoskeletal remodeling and transmigration in mice. *J Immunol*. 2020;205(2):521–532. doi:10.4049/jimmunol.1901054
22. Huang J, Qu H-P, Zheng Y-F, et al. The revised Atlanta criteria 2012 altered the classification, severity assessment and management of acute pancreatitis. *Hepatobiliary Pancreat Dis Int*. 2016;15(3):310–315. doi:10.1016/S1499-3872(15)60040-6
23. Banks PA, Bollen TL, Dervenis C, et al. Classification of acute pancreatitis--2012: revision of the Atlanta classification and definitions by international consensus. *Gut*. 2013;62(1):102–111. doi:10.1136/gutjnl-2012-302779
24. Zhu Q, Lin X, Liu X, et al. Dynamic changes of proteasome and protective effect of bortezomib, a proteasome inhibitor, in mice with acute pancreatitis. *Biochem Biophys Res Commun*. 2018;505(1):126–133. doi:10.1016/j.bbrc.2018.09.066
25. Love MI, Huber W, Anders S. Moderated estimation of fold change and dispersion for RNA-seq data with DESeq2. *Genome Biol*. 2014;15(12):550. doi:10.1186/s13059-014-0550-8
26. Ogata H, Goto S, Sato K, et al. KEGG: Kyoto Encyclopedia of Genes and Genomes. *Nucleic Acids Res*. 1999;27(1):29–34. doi:10.1093/nar/27.1.29
27. Stoimenou M, Tzoros G, Skendros P, et al. Methods for the assessment of NET formation: from neutrophil biology to translational research. *Int J mol Sci*. 2022;23(24):15823. doi:10.3390/ijms232415823
28. Sorensen OE, Borregaard N. Neutrophil extracellular traps - the dark side of neutrophils. *J Clin Invest*. 2016;126(5):1612–1620. doi:10.1172/JCI84538
29. Zha C, Meng X, Li L, et al. Neutrophil extracellular traps mediate the crosstalk between glioma progression and the tumor microenvironment via the HMGB1/RAGE/IL-8 axis. *Cancer Biol Med*. 2020;17(1):154–168. doi:10.20892/j.issn.2095-3941.2019.0353
30. Mattke J, Darden CM, Lawrence MC, et al. Toll-like receptor 4 in pancreatic damage and immune infiltration in acute pancreatitis. *Front Immunol*. 2024;15:1362727. doi:10.3389/fimmu.2024.1362727
31. Brinkmann V, Zychlinsky A. Beneficial suicide: why neutrophils die to make NETs. *Nat Rev Microbiol*. 2007;5(8):577–582. doi:10.1038/nrmicro1710
32. Dömer D, Walther T, Möller S, et al. Neutrophil extracellular traps activate proinflammatory functions of human neutrophils. *Front Immunol*. 2021;12:636954. doi:10.3389/fimmu.2021.636954
33. Ding Z, Deng Z, Li H. Single-cell transcriptome analysis reveals the key genes associated with macrophage polarization in liver cancer. *Hepatol Commun*. 2023;7(11). doi:10.1097/HC9.0000000000000304

34. Tarrant JM, Robb L, van Spriel AB, et al. Tetraspanins: molecular organisers of the leukocyte surface. *Trends Immunol*. 2003;24(11):610–617. doi:10.1016/j.it.2003.09.011
35. Higgins CB, Adams JA, Ward MH, et al. The tetraspanin transmembrane protein CD53 mediates dyslipidemia and integrates inflammatory and metabolic signaling in hepatocytes. *J Biol Chem*. 2023;299(2):102835.
36. Hsu AT, Bugajev V, Gottschalk TA, et al. Tetraspanin CD53 promotes inflammation but restrains mucus production in a mouse model of allergic airway inflammation. *Allergy*. 2024.
37. Tippett E, Cameron PU, Marsh M, Crowe SM. Characterization of tetraspanins CD9, CD53, CD63, and CD81 in monocytes and macrophages in HIV-1 infection. *J Leukoc Biol*. 2013;93(6):913–920.
38. Beinert T, Münzing S, Possinger K, et al. Increased expression of the tetraspanins CD53 and CD63 on apoptotic human neutrophils. *J Leukoc Biol*. 2000;67(3):369–373. doi:10.1002/jlb.67.3.369
39. Zhang F, Xia Y, Su J, et al. Neutrophil diversity and function in health and disease. *Signal Transduct Target Ther*. 2024;9(1):343.
40. Mollinedo F, Martín-Martín B, Gajate C, Lazo PA. Physiological activation of human neutrophils down-regulates CD53 cell surface antigen. *J Leukoc Biol*. 1998;63(6):699–706.
41. Khan MA, Palaniyar N. Transcriptional firing helps to drive NETosis. *Sci Rep*. 2017;7(1):41749. doi:10.1038/srep41749
42. Douda DN, Khan MA, Grasemann H, Palaniyar N. SK3 channel and mitochondrial ROS mediate NADPH oxidase-independent NETosis induced by calcium influx. *Proc Natl Acad Sci U S A*. 2015;112(9):2817–2822.
43. Weichhart T, Säemann MD. The PI3K/Akt/mTOR pathway in innate immune cells: emerging therapeutic applications. *Ann Rheum Dis*. 2008;67 (Suppl 3):p.iii70–4.
44. Guo G, Liu Z, Yu J, et al. Neutrophil function conversion driven by immune switchpoint regulator against diabetes-related biofilm infections. *Adv Mater*. 2024;36(8):e2310320. doi:10.1002/adma.202310320
45. Zhu CL, Xie J, Zhao -Z-Z, et al. PD-L1 maintains neutrophil extracellular traps release by inhibiting neutrophil autophagy in endotoxin-induced lung injury. *Front Immunol*. 2022;13:949217. doi:10.3389/fimmu.2022.949217